Poster P-201 has been designated as a Distinguished Poster at Display Week 2025. The full-length version of this paper appears in a Special Section of the *Journal of the Society for Information Display (JSID)* devoted to Display Week 2025 Distinguished Papers. This Special Section will be freely accessible until December 31, 2025 via:

https://sid.onlinelibrary.wiley.com/doi/full/10.1002/jsid.2089

Authors that wish to refer to this work are advised to cite the full-length version by referring to its DOI:

https://doi.org/10.1002/jsid.2089

Alignment Layer Optimization for Electrically Suppressed Helix Ferroelectric Liquid Crystals

Zhao-Yi CHEN[*$], Vigneshwaran Swaminathan*, Chris Mathew*, Valerii Vashchenko*, and Abhishek. K. Srivastava*[&]*

*** State Key Laboratory of Advanced Displays and Optoelectronics Technologies, and Center for Display Research, Department of Electronics and Computer Engineering, Hong Kong University of Science and Technology, Clear Water Bay Road, Kowloon, Hong Kong.**

[$]zchenhq@connect.ust.hk, eeswaminav@ust.hk, cmathew@connect.ust.hk, eevvv@ust.hk, [&]*eeabhishek@ust.hk*

Abstract

The Electrically Suppressed Helix Ferroelectric Liquid Crystal (ESHFLC) provides fast response at lower voltages and superior optical contrast, making it a promising choice for contemporary displays. Nevertheless, the constrained alignment techniques have hindered the commercialization of ESHFLC displays. To address this, we have optimized a polyimide (PI) based alignment layer by analyzing different PI concentrations and ESH diffraction to keep a balance between anchoring energy and elastic energy.

Keywords

Electrically suppressed helix, Ferroelectric liquid crystal, PI alignment

1. Introduction

The evolving needs of the community now center around high-resolution displays that push the boundaries of human visual acuity, low power consumption, and cost-effective devices. This presents a significant challenge for scientists and engineers alike. Ferroelectric Liquid Crystals (FLCs) have therefore attracted a lot of interest due to their quick response time and effectiveness, making them a desirable choice for modern display systems and photonic applications (1-3).

The electrically suppressed helix (ESH) FLC is a type of FLC mode that offers fast response at lower voltages and great optical contrast (4). The optimal cell gap and pitch ratio for ESHFLC indicate the crucial need for a delicate equilibrium between the surface anchoring energy and the helical elastic energy of the FLC molecules (5). This equilibrium plays a vital role in mitigating inherent defects linked to surface-stabilized FLC (SSFLC), including zig-zag defects stemming from chevron structures and defects arising from ferroelectric domains (6). Consequently, the optical quality of ESHFLC surpasses that of SSFLC, with a better contrast ratio (CR) and commendable mechanical stability. In 2015, a full-color display was developed using ESHFLC technology, achieving a color gamut that covers up to 130% of the NTSC requirements. This display operates on a field sequential mode that eliminates the need for a color filter, thereby enhancing efficiency (7).

However, limited alignment methods are holding back the commercialization of ESHFLC displays. Two most common alignment layer used for ESHFLC are Nylon 6 (N6) based on physical rubbing and Azodye based photoalignment layer (SD1). However, both above-mentioned alignment technologies are not suitable for large scale production of ESHFLC based displays due to the reasons discussed below. SD1 exhibits instability in high humidity environments and tends to undergo reorientation under ultraviolet light and blue light in bright displays, resulting in decreased performance and reduced lifespan of liquid crystal devices (8). On the other hand, N6 is dissolved in 2,2,2 Trichloroethanol, the chlorinated solvent is harmful to environments and not suitable for industrial use.

In this work, we have identified and optimized a Polyimide (PI) based alignment layer which is already used in commercial displays for nematic liquid crystals. The high optical quality of the ESHFLC depends on a precise balance between helical elastic energy and surface anchoring energy (9). To adjust the anchoring energy, we have altered the PI concentration and analyze the diffraction of ESHFLC under different PI concentrations.

2. Experiment

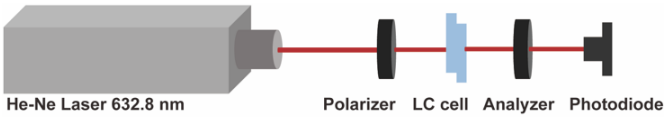

Figure 1. Experimental setup

The experiment was conducted within an optical setup comprising a laser (λ = 632.8 nm), Glan-Thompson cross-polarizers, a heating stage, and a photodetector. The ESHFLC molecules were in a planar alignment by utilizing an alignment layer with varying concentrations of PI. Additionally, the diffraction experiment doesn't need analyzer. A black background was placed behind the liquid crystal cell to observe the diffraction pattern. Furthermore, based on the POM images captured under a non-orthogonal polarizing microscope, the distribution of the diffraction period was calculated.

3. Results and Discussions

The PI concentration plays an important role in the alignment quality of ESHFLC. Fig. 2a shows six PI concentrations (The original concentration is given by 100 % and the other concentration mentioned are dilution of original concentration with NMP solvent) used as alignment layers in 1.7 μm cells with ITO glasses and the ESH material used for this study is FLC-11-165 (spontaneous polarization P_s=50 nC/cm^2, tilt angle θ=22.5°, rotational viscosity γ_ϕ=0.057 Pa·s, elastic energy K=2×10^{-11} N, helix pitch P_0=517 nm at 25 ℃). CR is one of the key indicators of ESHFLC in display applications. Fig. 2b and 2c illustrate the correlation between CR and PI concentration and the respective POM images are shown. In this case, the 41% concentration shows the highest CR of 6800:1 and other concentrations also exceeding 5500:1. In Fig. 2c, in the absence of an electric field, sizes of two domains in POM images change with different concentrations. It was further noted that the highest alignment quality aligns with the equal areas occupied by the two domains within the FLC cell texture.

ISSN 0097-996X/25/5603-2172-$1.00 © 2025

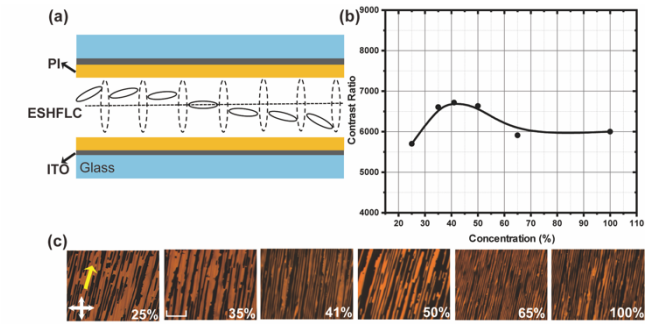

Figure 2. (a) The schematic of ESHFLC cells. (b) The CR of ESH with PI concentrations (25%, 35%, 41%, 50%, 65% and 100%). (c) POM images of ESH with six PI concentrations. White arrows are crossed polarizer, red arrow is rubbing direction and the scale bar is 40 μm.

Optimal contrast ratios are achieved when the anchoring energy from the alignment layer is comparable to, albeit slightly less than, the elastic energy of the FLC material. Moreover, Fig. 3 and Fig. 4a shows the response time of ESH at 10V is 22 μs while Fig. 4b illustrates the normalized transmittance of the cell under crossed polarized state using 632.8 nm laser as light source, saturating at 2V.

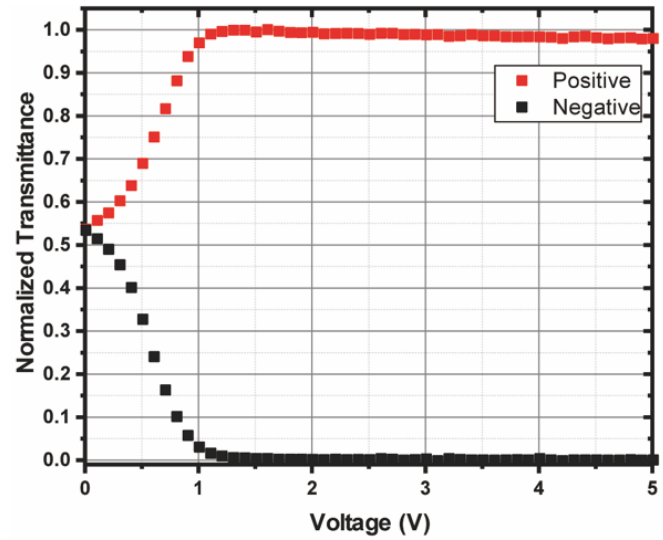

Figure 3. Transmittance plot against the applied electric field of ESH with 41% PI concentration.

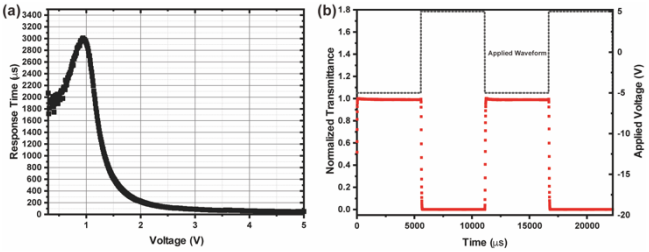

Figure 4. (a) The response time of ESH with 41% PI concentration. (b) Response curve of ESHFLC with 41% PI concentration at 90 Hz, 5 V.

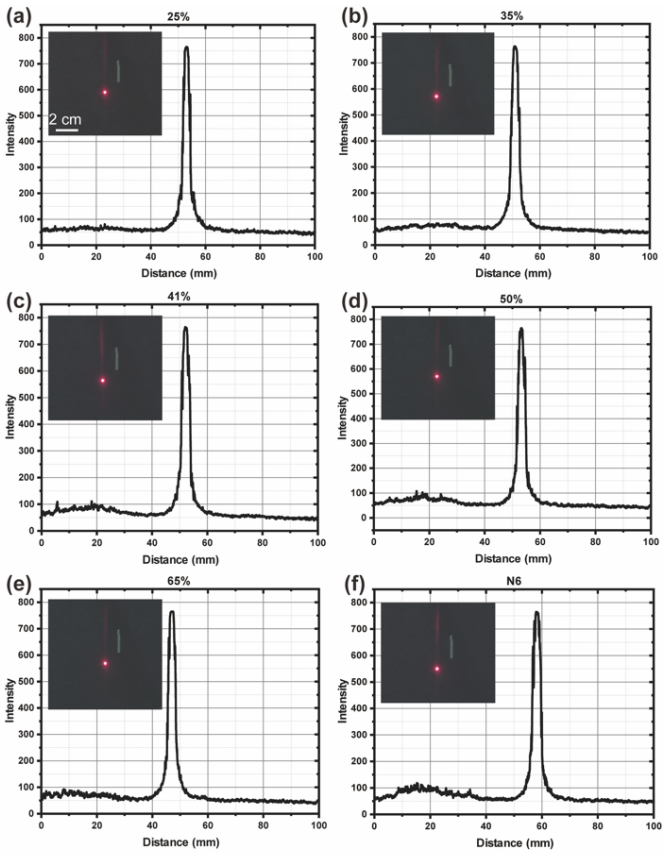

Figure 5. The diffraction intensity and pattern under five PI concentrations and 0.5% N6.

Additionally, the optical quality of ESHFLC can also be reflected by its diffraction characteristics. When the anchoring energy and elastic energy are balanced, ESHFLC should not exhibit diffraction at 632.8nm. As shown in Fig. 5, although unexpected diffraction patterns exist in ESHFLC with different concentrations of PI, the overall diffraction efficiency is less than 2% for all PI concentrations. The 0.5% N6 is also used as the alignment layer for the same ESHFLC material and cell gap. Additionally, the diffraction intensity of ESHFLC for each PI concentration is below N6, further illustrating the advantages of using this PI for ESHFLC displays.

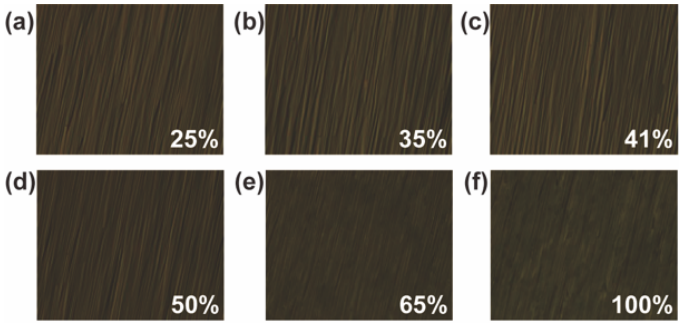

Figure 6. The POM images of ESHFLC with six PI concentrations under uncrossed polarizer at 0.1 Hz, % 5V.

Table 1. The calculated diffraction period of ESHFLC with six PI concentrations.

PI Concentration (%)	25	35	41	50	65	100
Diffraction period (μm)	5.02	5.51	4.79	4.67	4.53	4.24

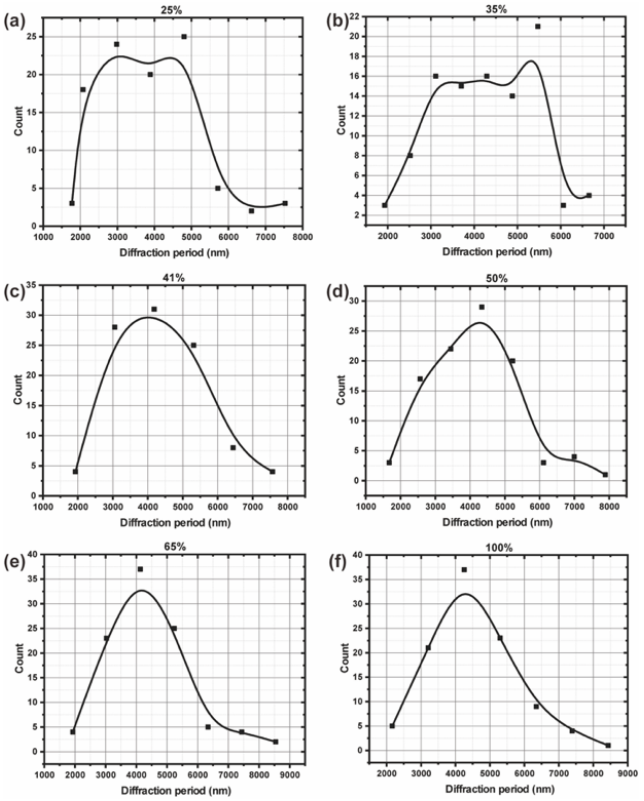

Figure 7. Diffraction periods with six PI concentrations measured by Image J based on POM images.

To analyze the origin of these diffraction patterns, in Table. 1, we calculated the diffraction periodicity of ESHFLC at each PI concentration based on the formula $\Lambda = \lambda/sin\theta$ (Λ is period, θ is diffraction angle). Furthermore, we measured the actual periodic distribution using Image J through the texture observed under a non-orthogonal polarizing microscope. Fig. 6 depicts the POM image captured under a non-orthogonal polarizing microscope, showing linear alternations of brightness. The diffraction of ESH may be related to the periodic lines of brightness alternation. We calculated the distribution of these line widths using Image J, as shown in Fig. 7. Different PI concentrations cause varied period distributions.

In Fig. 7, the distribution of diffraction periodicity of ESHFLC also varies with the concentration of PI. The peak width of the distribution curve decreases as the PI concentration increases. A narrower diffraction periodicity bandwidth can reflect an enhancement of the diffraction phenomenon, thereby further manifesting in an increase in the magnitude of diffraction intensity. Under the influence of 25% PI concentration, ESHFLC exhibits the widest diffraction periodicity bandwidth, corresponding to relatively lower diffraction intensity.

The diffraction pattern is likely caused by an imbalance between anchoring energy and elastic energy. In the ESH mode, the equilibrium between the elastic energy associated with the twisting of the FLC helix and the normalized anchoring energy across the cell gap due to the alignment layer allows for the external electric field to constrain the helix cone, resulting in uniform bright and dark states corresponding to the two polarities of the electric field applied. The elastic constant and anchoring energy can calculated using formulas $E_u=(\frac{\pi^2}{16})(\frac{K_{22}q_0^2}{P_s})$ and $\tau_A=\gamma_\varphi d/4W_Q$, where K_{22} is the elastic constant, q_0 represents the wave vector of the helix, given by $q_0=\frac{2\pi}{p_0}$, and W_Q is the anchoring energy. In the case where PI is used as the alignment layer at a concentration of 41%, the induced anchoring energy is approximately a quarter of the elastic energy that this ESHFLC possesses, leading to unexpected diffraction occurrences. To minimize such diffraction effects, it is possible to lower the elastic energy by altering the material's spontaneous polarization P_s, thus achieving a balance between two energies.

4. Conclusions

Overall, this PI can mitigate the industrial constraints imposed by N6 and SD1, including optical instability and environmental unfriendliness. Moreover, when utilized as an alignment layer, ESHFLC demonstrates excellent contrast ratio (up to 6800:1) and response time (22 μs). Unintended diffraction effects can also be eliminated by further adjusting the balance between anchoring energy and elastic energy. There is potential for its application in the large-scale production of ESH displays in the industry.

Acknowledgements

This work is supported by the Research Grants Council (RGC) of Hong Kong SAR (Nos. 26202019 and 16205623), an Innovation and Technology Commission (ITC) grant, ITS/059/22MX, and the funding for The State Key Laboratory of Advanced Displays and Optoelectronics Technologies, Hong Kong University of science and technology, Hong Kong.

References

1. Srivastava AK, Chigrinov VG, Kwok HS. Ferroelectric liquid crystals: Excellent tool for modern displays and photonics. Journal of the Society for Information Display. 2015;23(6):253-72.
2. Swaminathan V, Vashchenko V, Vashchenko O, Bhadra D, Mathew C, Kwok H-s, et al. 7-2: Truly Bi-stable Ferroelectric Liquid Crystal Based Modulators. SID Symposium Digest of Technical Papers. 2024;55(1):49-52.
3. Sun Z-B, Yuan Z-N, Swaminathan V, Vashchenko V, Vashchenko O, Cheung AYL, et al. Reconfigurable Geometrical Phase Spatial Light Modulator Using Short-Pitch Ferroelectric Liquid Crystals. Advanced Optical Materials. 2023;11(19):2300561.
4. Guo Q, Yan KX, Chigrinov V, Zhao HJ, Tribelsky M. Ferroelectric Liquid Crystals: Physics and Applications. Crystals. 2019;9(9).
5. Lapanik V, Bezborodov V, Sasnouski G, Haase W. Thin ferroelectric liquid crystal layers: mechanical stability and fast electro-optical response, connection between molecule design and surface properties. Liquid Crystals. 2013;40(10):1391-7.
6. Khan S, Prakash J, Chauhan S, Choudhary A, Biradar AM. Weak anchoring resolved substrate interface and bulk mode processes in surface stabilized ferroelectric liquid crystal. Journal of Molecular Liquids. 2021;325.
7. Srivastava AK, Chigrinov VG, Kwok HS. Electrically suppressed helix ferroelectric liquid crystals for modern displays.

Journal of the Society for Information Display. 2015;23(4):176-81.
8. Chigrinov V, Pikin S, Verevochnikov A, Kozenkov V, Khazimullin M, Ho J, et al. Diffusion model of photoaligning in azo-dye layers. Physical Review E. 2004;69(6):061713.
9. Hirosawa I. Method of characterizing rubbed polyimide film for liquid crystal display devices using reflection ellipsometry. Japanese Journal of Applied Physics Part 1-Regular Papers Short Notes & Review Papers. 1996;35(11):5873-5.